

2017:00021 - Unrestricted

# Report

## Thermal Properties of Organic Foods

DSC analysis of apple, carrot, pork, salmon and salmon oil

### Authors

Michael Bantle

Ignat Tolstorebrov, Norwegian University of Science and Technology



# Report

## Thermal Properties of Organic Foods

DSC analysis of apple, carrot, pork, salmon and salmon oil

**KEYWORDS:**Organic products  
Thermal properties  
Specific heat capacity  
Enthalpy  
Phase transition  
Glass transition  
Ice formation  
Freezing point**VERSION**

No1.

**DATE**

2017-02-07

**AUTHOR(S)**Michael Bantle, SINTEF Energy Research  
Ignat Tolstorebrov, Norwegian University of Science and Technology**CLIENTS**

ERA-NET and NFR

**CLIENT'S REF.**

SusOrganic /NFR247220

**PROJECT NO.**

SusOrganic 502000972

**NUMBER OF PAGES/APPENDICES:**

17 + Appendices

**ABSTRACT**

Thermal properties of selected organic products were investigated using novel DSC technique and methods of determination. The report includes determination of freezing temperatures, glass transition temperatures, amount of ice, and end of freezing point, heat capacity and thermal conductivity for selected cases. One part of the experimental work was devoted to investigate the difference between oils extracted from organic and conventional salmon.

The main aim of the investigation was to understand if the organic food requires any special treatment during processing, when compared with industrially produced foods.

For the investigated organic products (carrots, apples, salmon fillets and pork chops) no significant difference was found compared to conventional products. Organic salmon oil showed a different melting and freezing behaviour, which can be explained by the different fatty acid composition of the feed.

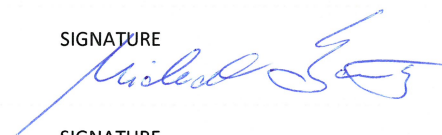
The performed investigation indicate that organic products can be preserved by the same technologies of the food chain than conventional products.

The determined data from the DSC analysis are available for download on <http://www.orgprints.org/>

**PREPARED BY**

Michael Bantle

## SIGNATURE

**CHECKED BY**

Ingrid Camilla Claussen

## SIGNATURE

**APPROVED BY**

Petter E. Røkke

## SIGNATURE

**REPORT NO.**

2017:00021

**ISBN**

978-82-14-06706-4

**CLASSIFICATION**

Unrestricted

**CLASSIFICATION THIS PAGE**

Unrestricted

# Document history

---

<b>VERSION</b>	<b>DATE</b>	<b>VERSION DESCRIPTION</b>
No1.	2017-02-07	Summary of the performed DSC investigations on apples, carrots, salmon and pork meat

# Table of contents

<b>1</b>	<b>Introduction .....</b>	<b>4</b>
<b>2</b>	<b>Materials and methods.....</b>	<b>5</b>
2.1	Characterization of the raw material.....	5
2.2	Sample preparation for experiment .....	6
2.3	Determination of the thermal properties.....	6
2.3.1	Description of experiment.....	6
2.3.2	Determination of end of freezing point.....	7
2.3.3	Determination of ice content .....	7
2.3.4	Determination of glass transition .....	9
2.3.5	Extraction of oils .....	9
2.3.6	Determination of Liquid fraction of oils at different temperatures .....	10
2.3.7	Statistical analysis.....	10
<b>3</b>	<b>Results and discussion .....</b>	<b>11</b>
3.1	Thermal properties of apples.....	11
3.2	Thermal properties of carrots.....	12
3.3	Thermal properties of pork.....	12
3.4	Thermal properties of salmon .....	13
3.1	Thermal properties of salmon's oils .....	13
<b>4</b>	<b>Conclusions .....</b>	<b>16</b>
<b>5</b>	<b>References .....</b>	<b>17</b>
	<b>Appendixes.....</b>	<b>18</b>

## 1 Introduction

Thermal properties of food products is one of the most important parameters, which is used for designing processing and storage conditions.

This study focuses on the following thermal properties of the selected foods:

- Glass transition temperature. Glass transition is a second order phase transitions, which occurs in food products with a high moisture content at low and ultra-low temperatures. This is solid phase of the material, but the matter is not structured as it happens in the case of crystalline state. Glass transition occurs at conditions, when ice formation is not possible in the system and high viscosity is observed (more than  $10^{12}$  Pa\*s) (Champion, Le Meste, & Simatos, 2000). This state is characterized by low molecular mobility, and it is considered that the product is very stable for long term storage at these conditions. The mechanical structure, on the other hand, is characterized by brittleness and high Young's modulus. The glass transition temperature depends on the chemical composition i.e. average molecular weight;
- End of freezing temperature. This temperature refers to conditions when the ice formation does not happen in the product when the temperature is further decreased. The formation of so-called maximum freeze concentration solution happens. This temperature helps to understand the preferable storage temperatures, that is when further decreasing of the temperature do not result in further increasing of the solid fraction and extra stability of the product;
- Unfreezable water. It is considered, that all freezable water is in the solid state below  $-40$  °C and only unfreezable water remains in the system as a liquid (Heldman, 1974). The unfrozen solution in muscles and tissues is complicated and contains of protein, fats, sugars, salt ions, droplets of fat etc. The amount of unfreezable water is quite significant and reaches up to 40 % from the protein weight (Schwartzberg, 1976). Thus, different deteriorative reactions may occur at temperatures below  $-40$  °C. The knowledge of unfreezable water and end of freezing help to understand amount of ice in the product with respect to the freezing temperature, which is extremely important when designing the freeze-drying methods and storage conditions for foods;
- Investigation of the fish oil properties. The glass transition of the fish oils was detected at temperatures below  $-110.0$  °C (Tolstorebrov et al, 2014). This means that some amount of the fish oil stays in a liquid supercooled state at ultra-low temperatures. The melting of the fish oils will be different due to peculiarities in composition. The determination of a solid fraction in fish oils at different temperatures by DSC is beneficial. It is possible to obtain the melting thermogram during one investigation. Consequently, the solid fraction content can be calculated by the partial integration of the melting peaks.

The determination procedure of the thermal properties is introduced in the next section.

## 2 Materials and methods

### 2.1 Characterization of the raw material

All the raw material was obtained from the local market, Norway Trondheim. Examples of labelling are introduced in Figure 1.



Figure 1. Types of carrots and apples, which were used for experiments.

Table 1 and Table 2 show water content in raw material and their parts. The water content was higher in organic carrots ( $p < 0.05$ ) when compared with non-organic. At the same time, pork and salmon did not show any statistically significant difference in water contents. The lean meat of this species was investigated.



**Table 1. Water content in carrots and apples.**

	Apples		Carrots	
	Organic	Non-organic	Organic	Non-organic
<b>Whole</b>	85.1 (0.5)	85.8 (0.5)	92.9 (0.2)	90.8 (0.2)
<b>Core</b>	-	-	92.7 (0.2)	91.5 (0.2)
<b>Main tissues</b>	-	-	92.1 (0.2)	91.0 (0.2)
<b>Skin</b>	-	-	92.7 (0.2)	90.5 (0.2)

**Table 2. Water and fat content in pork and salmon**

	Pork		Salmon	
	Organic	Non-organic	Organic	Non-organic
<b>Tissues with low fat content</b>	74.0 (1.0)	74.5 (1.0)	70.6 (0.5)	71.0 (0.4)
<b>Fat in the tissues</b>	<4.0	<4.0	8.0 (0.5)	approx. 7.1 (0.3)

## 2.2 Sample preparation for experiment

Fresh samples were obtained directly from the product with a lancet to avoid the connective tissues. Then the samples were placed into plastic vials (50 mL) with hermetic lids and stored in the chilling chamber (Electrolux ERF3866AOX, Sweden) at  $+4.0 \pm 1.0$  °C.

## 2.3 Determination of the thermal properties

### 2.3.1 Description of experiment

The DSC analysis was done with a DSC Q2000 (TA Instruments, USA) equipped with a Liquid Nitrogen Cooling System (TA Instruments, USA). The temperature calibration was done with indium (2.53 mg) and water (2.85 mg). The heat capacity was calibrated with a sapphire in the range between  $-150.0$  °C and  $150.0$  °C. Helium was chosen as a purge gas at  $25$  mL  $\text{min}^{-1}$ , according to TA's instrument recommendations. The reference sample was an empty hermetically sealed aluminium pan (50.52 mg).

The samples with masses between 3 mg and 10 mg were placed into aluminium pans with hermetic lids. The pans were sealed with a Tzero® DSC Sample Encapsulation Press (TA Instruments, USA). This procedure helped to obtain a high quality of hermetic sealing. Then the samples were placed by an autosampler into the DSC cell.

Samples with a low moisture content (below 25.0 % w. b.) were cooled and equilibrated for 60 minutes at  $-150.0$  °C; the cooling rate was  $5$  °C  $\text{min}^{-1}$ . Then samples were heated to  $25.0$  °C with the heating rate of  $5$  °C  $\text{min}^{-1}$ . Samples with a high moisture content above 25.0 % w.b. were cooled ( $5$  °C  $\text{min}^{-1}$ ) and equilibrated at  $-150.0$  °C for 60 minutes, then warmed up to  $-40.0$  °C ( $5$  °C  $\text{min}^{-1}$ ) and equilibrated for 60 minutes and cooled again to  $-150.0$  °C ( $5$  °C  $\text{min}^{-1}$ ). Such equilibration at higher temperatures after chilling is called annealing in

the literature. The annealing is considered to be helpful for achieving the maximal freeze concentration  $a$ , as a consequence, avoiding exothermic peaks. But some researchers reported a glass transition in fish meat without annealing (Agustini et al., 2001; Inoue & Ishikawa, 1997; Ohkuma et al., 2008). Exothermic peaks during heating are mostly associated with the recrystallization of existing crystals, and can be found in products which contain carbohydrates or fats. For example, perfect exothermic peaks have appeared in dried tomatoes after a glass transition (Telis & Sobral, 2002). The DSC scanning to 25.0 °C was performed at the rate of 10 °C min<sup>-1</sup> as in the low moisture content samples. Each point was analysed in 5 replicates.

Fish oils were investigated following the same experimental setup, but without annealing. The cooling rate was 0.2 °C min<sup>-1</sup> (Tolstorebrov, Eikevik, & Bantle, 2014a) This is very important to maintain such rate of cooling to avoid formation of alfa-crystals of TAG. The DSC investigation of oils with alfa-structure will result in cold crystallization process, which influence negatively on determination of glass transition temperatures and solid fraction of oils at different temperatures.

### 2.3.2 Determination of end of freezing point

The determination of the onset of melting ( $T^m$ ), using the heat flow DSC curve, is complicated due to the gentle change in the slope of the heat flow. Assuming that the heat flow of a substance not undergoing phase transition should be continuous, one can state that the derived heat flow would follow a linear trend. The detectable deviation from such trend represented the thermal transition in the substance. The changes mentioned above were detected on the derived heat flow curve derived for each of the investigated fish species in the same temperature range, as shown in Figure 2.

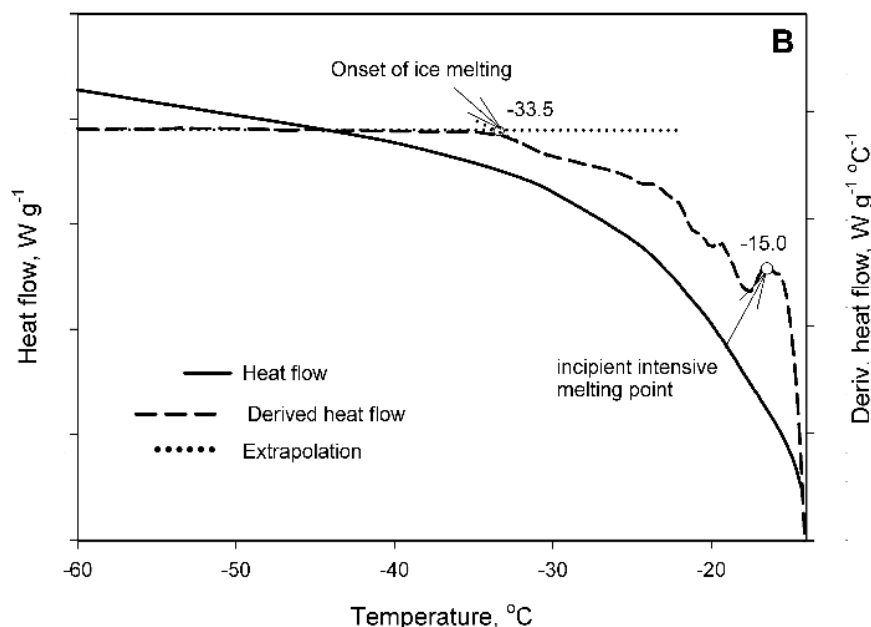


Figure 2. Example of end point office formation determination (onset of ice melting).

### 2.3.3 Determination of ice content

The amount of unfreezable water was detected by the DSC melting curve analysis. The DSC melting peaks, Figure 3, were integrated with the sigmoidal tangent baseline function. Straight baselines were drawn from



each limit, and an S-shaped curve was drawn to connect the two baselines before and after the transition. The shape of the curve was obtained by taking into account the slope of the heating curve before and after the ice melting peak.

The rough estimation of the ice's mass of ice was calculated by the following Eq. 1 (Kumagai, Nakamura, & Fujiwhara, 1985):

$$I = \frac{E_{product}}{L_{ice}} \quad (1)$$

$L_w = 333.55 \text{ kJ kg}^{-1}$  at  $0 \text{ }^\circ\text{C}$ . The enthalpy of ice melting depends on temperature. This leads to an underestimation of the ice quality quantity at temperatures below  $0 \text{ }^\circ\text{C}$ . For correction purposes, the empirical equation suggested by Riedel (1978) was used:

$$L_{ice} = 333.5 + 2.05 * T_m - 4.19 * 10^{-3} T_m^2 \quad (2)$$

This equation describes the change of the heat of fusion with temperature accurately. In accordance with this, the ice fraction was estimated using Eq. 1 modified by Eq. 2:

$$x_{ice} = \frac{\int_{T_m}^{T_f} I dT}{\int_{T_m}^{T_f} I dT} \quad (3)$$

The  $dT$  was  $0.0165 \text{ }^\circ\text{C}$ . The amount of unfreezable water was obtained as the difference between the total water fraction in the product and the ice fraction.

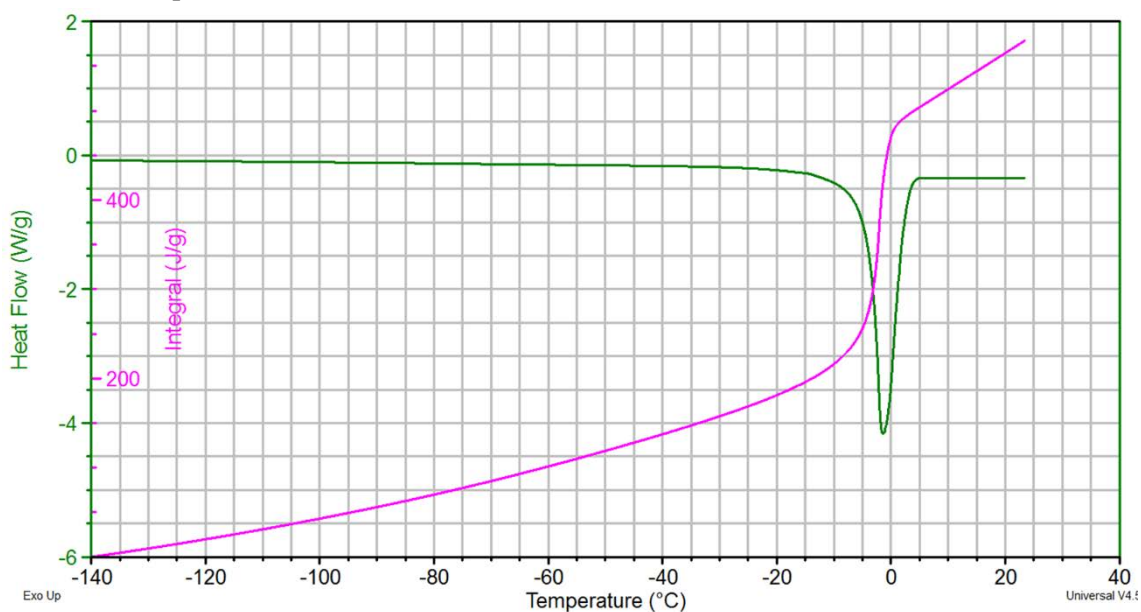


**Figure 3. Example of heat flow curve (green) with melting peak and its integration (rose) – the enthalpy curve.**

### 2.3.4 Determination of glass transition

The glass transition was determined with TA Universal Analysis 2000 version 4.5A software (TA instruments, USA). The glass transition was characterized with the following parameters of the endothermic baseline shift: the onset (T<sub>go</sub>), end (T<sub>ge</sub>) and inflection (T<sub>gi</sub>) points. The onset and end points were measured by an extrapolation of the baselines to the intersection with the glass transition line. Because the glass transition was detected by the heating of the sample, the end point refers to a higher temperature than the onset point. The inflection point shows the inflection of the glass transition curve, and was found as illustrated in Figure 4. This point should not be confused with the midpoint of the glass transition, which is measured as a middle point on the virtual glass transition line between the onset and end point of the glass transition. Also, the inflection point is characterized by a negative peak of the derived heat flow curve.

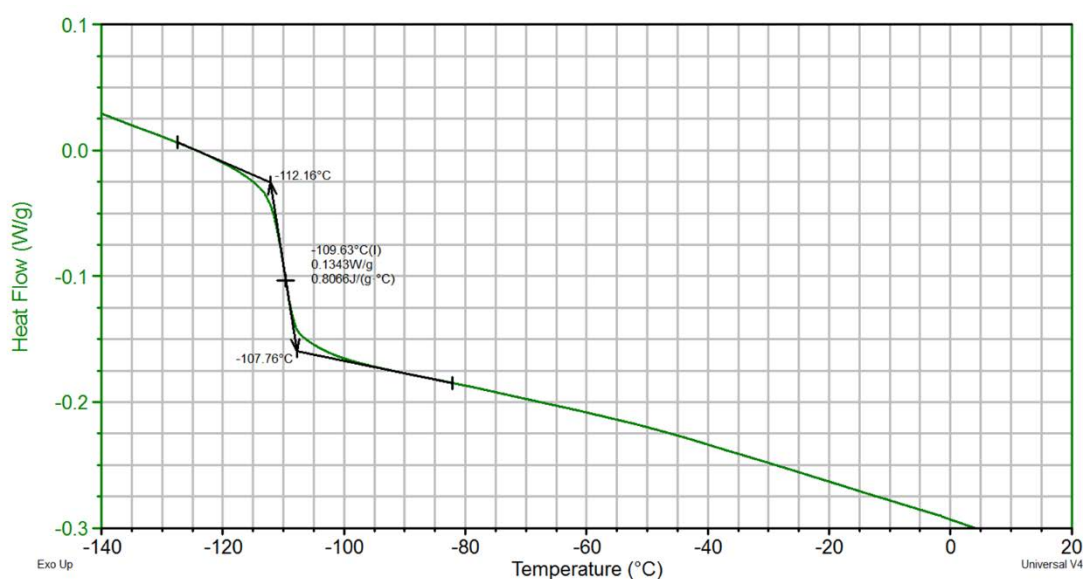


**Figure 4** Example of glass transition on heat flow curve.

### 2.3.5 Extraction of oils

The fat for DSC was extracted using a rapid method for lipid extraction (Bligh & Dyer, 1959):

1. Weigh tissue. Grind dry tissue in mortar and pestle.
2. Add tissue to glass tube, add 3 mls 2:1 MeOH:chloroform. Smash with glass rod.
3. Mix on Nutator 20 minutes.
4. Add 1 ml chloroform and 1.8 mls water.
5. Shake and Spin
6. Discard upper layer (aqueous phase, will contain some polar lipid species like acyl-CoAs)
7. Transfer lower layer (organic phase contains TAGs, membrane lipids and other neutral lipids) to new tube
8. Dry sample under inert atmosphere.
10. Dissolve in 200 ul 1:1 chloroform: methanol or 6:1 chloroform:methanol.

The fat samples were stored at  $-86.0 \pm 1.0$  °C (MDF chest freezer, Sanyo, Japan) before DSC. The oil was extracted from the average probe which was prepared with 5 fillets.

### 2.3.6 Determination of Liquid fraction of oils at different temperatures

TAGs, which compose fish oils, have different melting temperatures and different heats (enthalpies) of fusion (Walstra, 2003). Plotting the enthalpy of fusion against the melting temperature of different TAG's gives a non-linear trend, which describes the dependence between the enthalpy of fusion ( $\Delta H$ , [kJ kg<sup>-1</sup>]) and the melting temperature ( $T_m$  [°C]), Eq. 4 (Tolstorebrov et al., 2014a):

$$\Delta H = 2.08 * 10^{-6} * \left(\frac{1}{273.02+T_m}\right)^{-3.61} \quad (4)$$

The R<sup>2</sup> equals 0.91, F(Ratio)=242 and Prob(F)=0. Such quality parameters lead us to a positive conclusion concerning the validity of the model obtained.

The melted mass of oil ( $m$  [kg]) for an infinitely small temperature difference ( $\Delta=0.01$ K or less) was calculated as a ratio of the energy absorbed by the sample during melting ( $E_{T_2-T_1}$  [kJ]) to the average heat of fusion ( $\Delta H_{T_{av}}$ ) for this temperature range, Eq.5:

$$m_{T_2-T_1} = \frac{E_{T_2-T_1}}{\Delta H_{T_{av}}} \quad (5)$$

The melted mass at a given temperature can be found by Eq. 6:

$$m_T = \int_{T_{m,o}}^T m dT \quad (6)$$

Accuracy of this method is  $\pm 5.0$  %.

### 2.3.7 Statistical analysis

The analysis of variance (ANOVA: a single test and two-factor test with replication) was applied to analyse the obtained data. The difference was considered significant at  $p < 0.05$ .

The standard deviation is introduced in the brackets after the values given in the text.

### 3 Results and discussion

#### 3.1 Thermal properties of apples

The thermal properties of organic and non-organic apples are introduced in Table 3. It should be noted that only water content was analysed for these samples (see. Table 1). Statistically significant difference was not found for the water content between the two groups of samples ( $p>0.05$ ).

**Table 3. Thermal properties of organic and non-organic apples.**

Properties	Apples	
	Main tissues	Organic apples
End of freezing, °C	-43.42 (0.4) <sup>a</sup>	-44.34 (0.5) <sup>b</sup>
Glass transition $T_{g,i}$ , °C	-54.74 (2.5) <sup>c</sup>	-57.19 (2.5) <sup>c</sup>
Unfreezable water From total weight, %	3.0 % <sup>d</sup>	3.0 % <sup>d</sup>
Maximal freeze concentration, % of solids	83.30 (0.5) <sup>e</sup>	83.40 (0.5) <sup>e</sup>

Glass transition temperature, unfreezable water content and maximal freeze-concentration did not show any significant difference ( $p>0.05$ ) between the organic and non-organic samples. At the same time, the end of freezing point (incipient point of melting) showed statistical difference ( $p<0.05$ ). The ice formation in non-organic apples ends at a bit lower temperature, when compared with organic. The similar values for apples were obtained before by Bai et. al. (2001), when the incipient point for glass transition was found at  $-57.8$  °C, but end of freezing was detected at  $-50.3$  °C. Taking into account that the similar DSC method was used, we can conclude that such difference in the ice formation can be related with difference in carbohydrate composition of the apples.

Integration of the DSC melting peaks of fresh organic apples (see section 2.3.3.) was used to obtain the ice fraction in apple tissues at different temperatures, Figure 5.

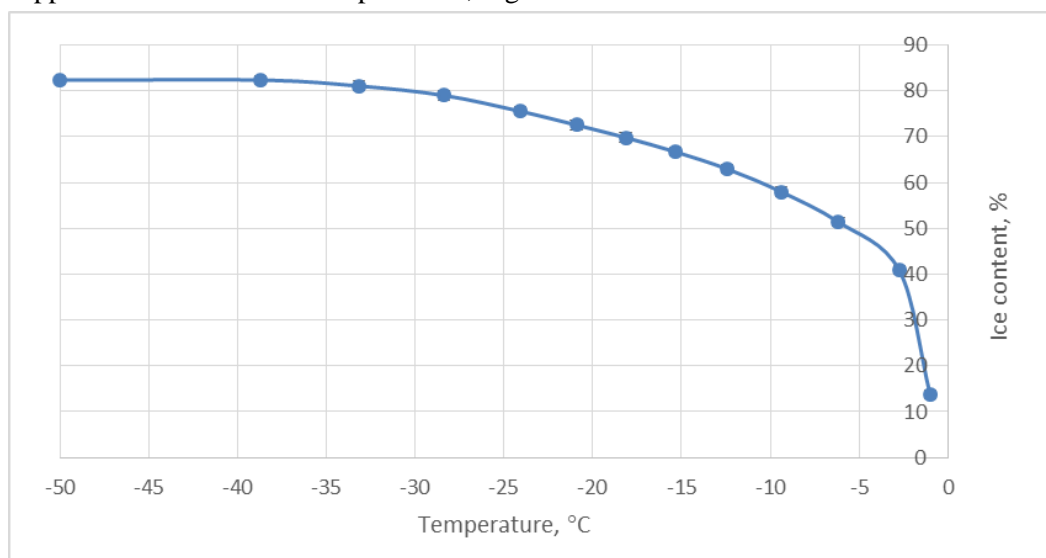


**Figure 5. Ice fraction in organic apples at different temperatures.**

The figure 5 shows the most intensive formation of ice crystals happens in the temperature range between the freezing point and -5.0 °C, when the ice fraction reaches 50% from the total weight of the product. Further decreasing of the temperature to -10.0 °C will result in increasing of ice fraction up to 60 % from the total weight of the sample. Thus, the vacuum-freeze drying of the organic apples can be done in the temperature diapason between -10.0 and -5.0 °C.

### 3.2 Thermal properties of carrots

Thermal properties of organic carrots are introduced in Table 4. The End point of freezing and glass transition temperature did not show any statistical difference between organic and non-organic carrots ( $p > 0.05$ ). At the same time, amount of unfreezable water was much lower, when compared with apples ( $p < 0.05$ ).

It is interesting to compare glass transition temperatures of carrot and apples. They appear at quite narrow temperature range between -52.0 and -57.0 °C. It shows that the maximal freeze concentrated solution has similar average molecular weight. But, amount of unfreezable water is significantly different ( $p < 0.05$ ). This means that different amount of solids (carbohydrates or proteins) take part in formation of the glassy matrix.

Previous investigation of carrots with a lower moisture content (88.0% w.b.) revealed unfreezable water at 8 % (determined by DSC) and 3.4 % determined by enthalpy difference method (Roos, 1986). The incipient point of melting was detected at -39.0 °C, which very close to our investigations.

**Table 4. Thermal properties of organic and non-organic carrots.**

Properties	Carrot			Organic carrot		
	core	main	skin	core	main	skin
End of freezing, °C	-42.0 (0.5)	-42.0 (0.5)	-42.0 (0.5)	-42.0 (0.5)	-42.0 (0.5)	-42.0 (0.5)
Glass transition $T_{g,i}$ , °C	-52.0 (0.8)	-52.0 (0.8)	-52.0 (0.8)	-53.0 (0.8)	-53.0 (0.8)	-53.0 (0.8)
Unfreezable water From total weight, %	2.23 (0.5)	2.52 (0.5)	2.29 (0.4)	1.27 (0.6)	0.83 (0.3)	3.08 (0.2)
Maximal freeze concentration, % of solids	79.18	77.90	75.94	87.03	91.13	77.04

### 3.3 Thermal properties of pork

The thermal properties of lean pork meat is introduced in Table 5. Glass transition, unfreezable water content and maximal freeze concentration of solids was similar for both types of samples ( $p > 0.05$ ). At the same time, the end of freezing point showed significant difference in its values between samples ( $p < 0.05$ ). However, such big difference does not result in any significant amount of ice, which will be formed in the temperature range between -25.77 and -30.67 °C (approx. 0.2 % form total weight of the sample).

The recent study of raw pork legs, which is used for Norwegian Jamon production, revealed glass transition at approx. -71.0 °C. Unfreezable water was also in the same range as for our research (Petrova, Tolstorebrov, Mora, Toldrá, & Eikevik, 2016).

**Table 5. Thermal properties of organic and non-organic pork**

Properties	Pork	Organic Pork
End of freezing, °C	-25.77 (1.0)	-30.67 (1.2)
Glass transition $T_{g,i}$ , °C	-70.92 (1.4)	-70.85(1.1)
Unfreezable water From total weight, %	7.8 (1.8)	7.8 (1.5)
Maximal freeze concentration, % of solids	75.00 (2.3)	74.00 (1.1)

### 3.4 Thermal properties of salmon

Thermal properties of organic and non-organic salmon did not give any statistically significant difference ( $p > 0.05$ ), Table 6. The same trend was observed for investigations of thermal properties for different types of fishes (Tolstorebrov, Eikevik, & Bantle, 2014b). It seems to be, that protein content influence on the amount unfreezable water and temperature of glass transition. The thermal properties of fish protein are similar irrespectively from origin.

**Table 6. Thermal properties of organic and non-organic salmon**

Properties	Salmon	Organic Salmon
End of freezing, °C	-29.33 (0.4)	-30.04 (0.4)
Glass transition $T_{g,i}$ , °C	-76.4 (1.2)	-75.9 (1.2)
Unfreezable water From total weight, %	6.61 (0.3)	6.64 (0.5)
Maximal freeze concentration, % of solids	75.00 (2.3)	74.85 (2.0)

### 3.1 Thermal properties of salmon's oils

Thermal properties of organic and non-organic salmon oils showed significant variations in properties. Especially, the significant difference was found in melting behaviour during DSC scanning, Figure 5. The glass transition of fish oils are found in different temperature range, but this is explained by presence of not evaporated solvent in non-organic (industrial) samples of salmon oil. The significant difference in the size of glass transition shift was observed between these two types of samples. Organic salmon showed less intensive shift on heat flow curve. The glass transition in fish oils is explained by presence of TAG, which are composed by omega-3 polyunsaturated fatty acids (see table 7). They remain liquid during freezing and do not form crystals even at long-term exposition at -86.0 °C.



The size of the glass transition shift on the heat flow curve is related to the amount of this unfreezable fraction in oils. As high shift as much omega3 polyunsaturated fatty acids is presented in the investigated sample. Thus, the amount of essential fatty acids is significantly reduced in the organic oils, because the shift is relatively small and moving.

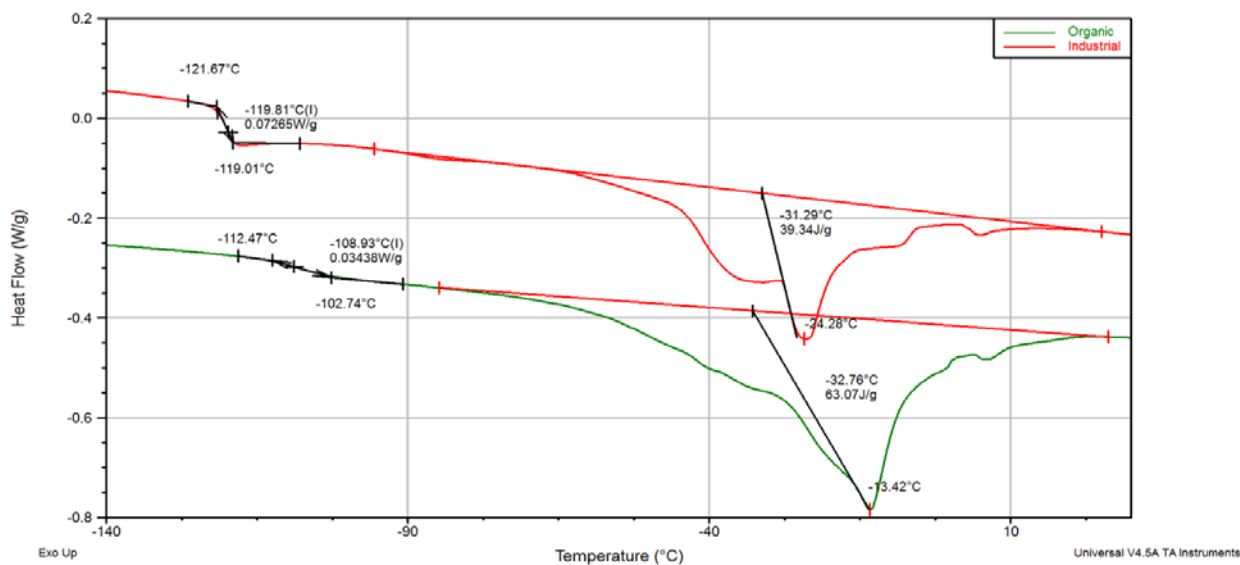


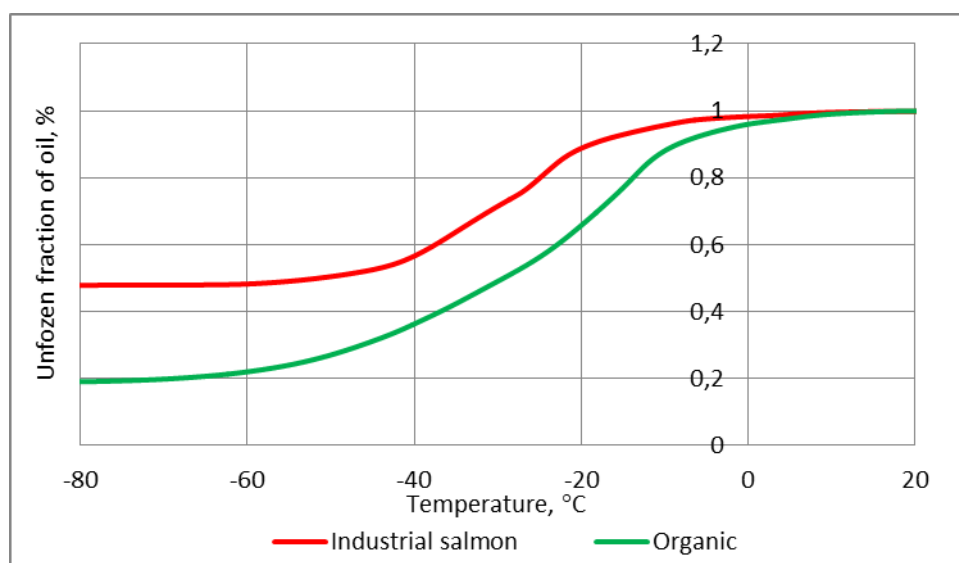
Figure 5. DSC heat flow curves for oils, which were extracted form organic (green) and non-organic (red) salmons

Table 7 – The glass transition in TAGs(Tolstorebrov et al., 2014a)

Nomenclature	Fatty acid	Abbreviation	Glass transition, °C		
			onset	inflection	end
<b>Tricosapentaenoin;</b> <b>1,2,3-tri-</b> <b>(5Z,8Z,11Z,14Z,17Z-</b> <b>icosapentaenoyl)-sn-glycerol</b>	C20:5 $\omega(5c,8c,11c,14c,17c)$	EPAx3	-113.89	-111.78	-109.5
<b>Tridocosahexaenoin;</b> <b>1,2,3-tri-</b> <b>(4Z,7Z,10Z,13Z,16Z,19Z-</b> <b>docosahexaenoyl)-sn-</b> <b>glycerol</b>	C22:6 $\omega(4c,7c,10c,13c,16c,19c)$	DHAx3	-113.04	-110.39	-108.7
<b>Trigammalinolenin;</b> <b>1,2,3-tri-(6Z,9Z,12Z-</b> <b>octadecatrienoyl)-sn-</b> <b>glycerol</b>	18:3 $\omega(6c,9c,12c)$	$\gamma$ Lix3	-111.85	-109.8	-108.22
<b>Triarachidonin;</b> <b>1,2,3-tri-(5Z,8Z,11Z,14Z -</b> <b>icosatetraenoyl)-sn-glycerol</b>	20:4 $\omega(5c,8c,11c,14c)$	AaAaAa	-110.38	-107.25	-105.59

The melting profiles of organic and non-organic salmon oils consist of one melting peak in the temperature range between -24.0 and -13.0 °C. The major part of the freezable fraction of fish oil will be frozen at temperatures below these values.

Unfrozen fraction of salmon oils was calculated based on DSC heat flow curve by method described by Tolstorebrov et.al. (2014a) (see section 2.3.6.). It was found that the non-organic salmon has a higher amount of unfreezable fraction 48.0 vs 20.0%. This can be explained by difference in feed composition. The fatty acid composition of the fish feed reflect on the fatty acids composition of fish oil (Baron, Hyldig, & Jacobsen, 2009).



**Figure 6. Comparisons of liquid fractions in oils with respect to temperature.**

At the same time, organic salmon is more stable to oxidation during storage when compared with non-organic, because the major part of the oil will be crystalline at low storage temperatures. The oxidative reactions belong to chain reactions (Kamal-Eldin & Yanishlieva, 2005), and the crystalline form of the oils can limit the propagation of the oxidative reaction due to the immobilization of the TAG molecules. However, further investigation and analysis of feeding is required.

## 4 Conclusions

Organic products are commonly associated with higher sustainability and an improved or at least different product quality compared to conventional products. The aim of the present investigation was to determine if the thermal properties of selected organic products are different from conventional products. The report includes determination of freezing temperatures, glass transition temperatures, amount of ice, and end of freezing point, heat capacity and thermal conductivity for selected cases. A part of investigation was devoted to investigation of the difference between oils extracted from organic and typical aquaculture salmon.

The determined data from the DSC analysis are available for download on <http://www.orgprints.org/>

Thermal properties of food are commonly used in food processing technology for design and dimensioning (e.g. refrigeration or chilled storage). To a certain extent they can also be used to determine the product quality, like in the present study when the amount of fatty acids is related to the freezing characteristic of salmon oil.

The investigated products were organic produced apples and carrots, as well as organic farmed salmon fillets and pork chop. The determined thermal properties were compared and benchmarked with conventional produced products.

The only significant difference was found for organic salmon oil, which showed a different melting and freezing behaviour. This can be explained by the different fatty acid composition of the feed.

All other investigations showed no statistically significant difference between organic and conventional produced apples, carrots and pork chops. For organic pork chop the end of freezing was approximately 5 Kelvin lower compared to conventional pork chop. However, this difference will not influence the amount of formed ice during freezing or the freezing process in general.

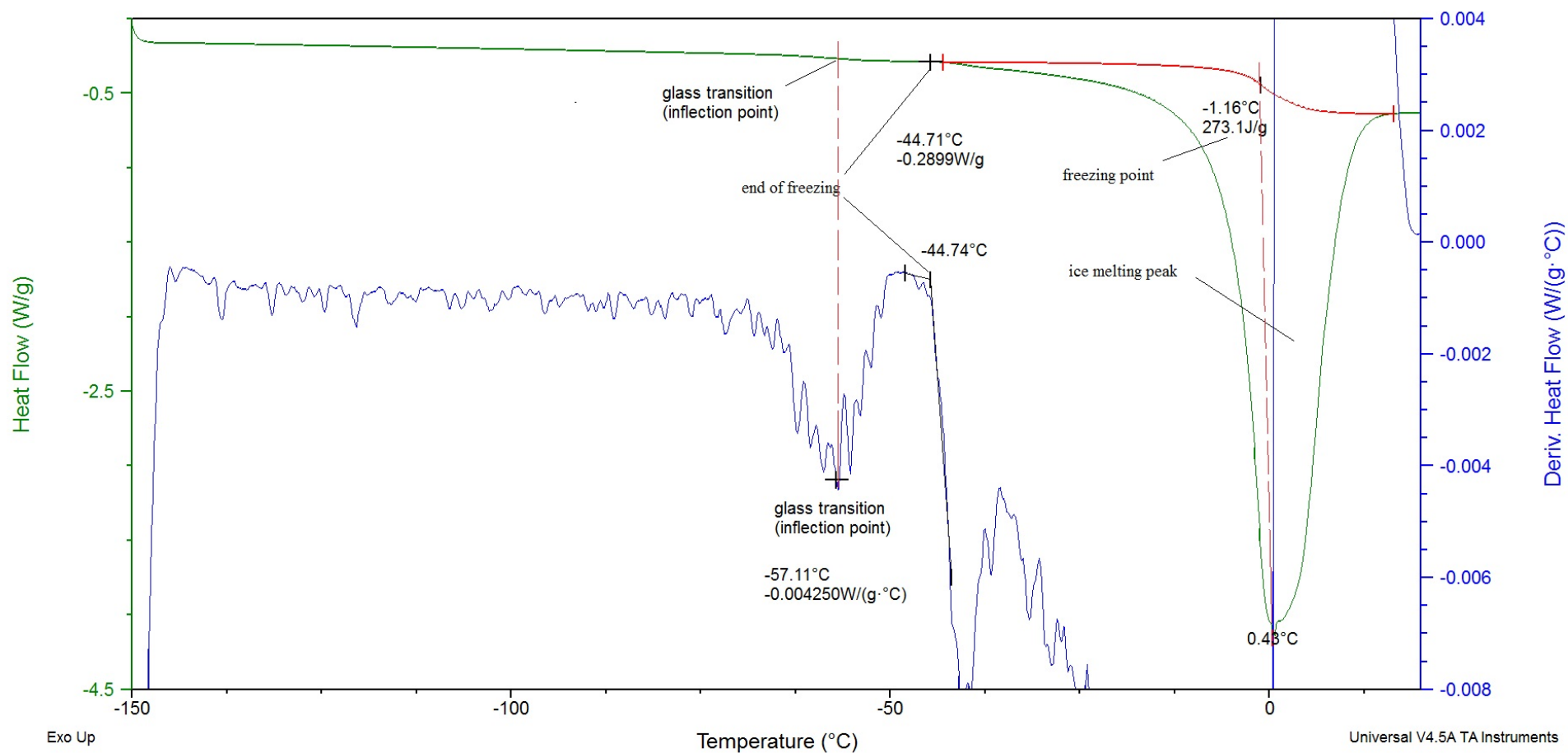
Summarized: The determined thermal properties for apples, carrots, salmon fillets and pork chop did not show a significant difference compared to conventional produced products. This result indicates that thermal processing of organic food, such as freezing, chilling, superchilling or drying, can be designed and applied under the same conditions like conventional food products. Hence, the requirements for the preservation conditions in the food chain are the same for organic products as for conventional products.

## 5 References

- Agustini, T. W., Suzuki, T., Hagiwara, T., Ishizaki, S., Tanaka, M., & Takai, R. (2001). Change of K value and water state of yellowfin tuna *Thunnus albacares* meat stored in a wide temperature range (20°C to -84°C). *Fisheries Science*, 67(2), 306-313. doi: 10.1046/j.1444-2906.2001.00226.x
- Bai, Y., Rahman, M. S., Perera, C. O., Smith, B., & Melton, L. D. (2001). State diagram of apple slices: glass transition and freezing curves. *Food Research International*, 34(2-3), 89-95. doi: [http://dx.doi.org/10.1016/S0963-9969\(00\)00128-9](http://dx.doi.org/10.1016/S0963-9969(00)00128-9)
- Baron, C. P., Hyldig, G., & Jacobsen, C. (2009). Does feed composition affect oxidation of Rainbow Trout (*Oncorhynchus mykiss*) during frozen storage? *Journal of Agricultural and Food Chemistry*, 57(10), 4185-4194. doi: 10.1021/jf803552h
- Champion, D., Le Meste, M., & Simatos, D. (2000). Towards an improved understanding of glass transition and relaxations in foods: molecular mobility in the glass transition range. *Trends in Food Science and Technology*, 11(2), 41-55. doi: 10.1016/s0924-2244(00)00047-9
- Heldman, D., R. (1974). Predicting the relationship between unfrozen water fraction and temperature during food freezing using freezing point depression. *Transactions of the ASABE.*, 17(1), 63-66.
- Inoue, C., & Ishikawa, M. (1997). Glass transition of tuna flesh at low temperature and effects of salt and moisture. *Journal of Food Science*, 62(3), 496-499. doi: 10.1111/j.1365-2621.1997.tb04414.x
- Kamal-Eldin, A., & Yanishlieva, N. (2005). Kinetic Analysis of Lipid Oxidation Data *Analysis of Lipid Oxidation* (pp. 234-262): AOCS Publishing.
- Kumagai, H., Nakamura, K., & Fujiwhara, J. (1985). DSC measurement of frozen water in liquid foods. *Agricultural and Biological Chemistry Journal*, 49(11), 3097-3101.
- Ohkuma, C., Kawai, K., Viriyarattanasak, C., Mahawanich, T., Tantratian, S., Takai, R., & Suzuki, T. (2008). Glass transition properties of frozen and freeze-dried surimi products: Effects of sugar and moisture on the glass transition temperature. *Food Hydrocolloids*, 22(2), 255-262. doi: 10.1016/j.foodhyd.2006.11.011
- Petrova, I., Tolstorebrov, I., Mora, L., Toldrá, F., & Eikevik, T. M. (2016). Evolution of proteolytic and physico-chemical characteristics of Norwegian dry-cured ham during its processing. *Meat Science*, 121, 243-249. doi: <http://dx.doi.org/10.1016/j.meatsci.2016.06.023>
- Riedel, L. (1978). Eine formel zur berechnung der enthalpie fettarmer lebensmittel in abh ngigkeit von wassergehalt und temperatur. *Bureau of Standards Journal of Research*, 5, 129-133.
- Roos, Y., H. (1986). Phase transitions and unfreezable water content of carrots, reindeer meat and white bread studied using Differential Scanning Calorimetry. *Journal of Food Science*, 51(3), 684-686. doi: 10.1111/j.1365-2621.1986.tb13911.x
- Schwartzberg, H. G. (1976). Effective heat capacities fro the freezing and thawing of food. *Journal of Food Science*, 41(1), 152-156. doi: 10.1111/j.1365-2621.1976.tb01123.x
- Telis, V. R. N., & Sobral, P. J. A. (2002). Glass transitions for freeze-dried and air-dried tomato. *Food Research International*, 35(5), 435-443. doi: 10.1016/s0963-9969(01)00138-7
- Tolstorebrov, I., Eikevik, T. M., & Bantle, M. (2014a). A DSC determination of phase transitions and liquid fraction in fish oils and mixtures of triacylglycerides. *Food Research International*, 58(0), 132-140. doi: <http://dx.doi.org/10.1016/j.foodres.2014.01.064>
- Tolstorebrov, I., Eikevik, T. M., & Bantle, M. (2014b). A DSC study of phase transition in muscle and oil of the main commercial fish species from the North-Atlantic. *Food Research International*, 55(0), 303-310. doi: <http://dx.doi.org/10.1016/j.foodres.2013.11.026>
- Walstra, P. (2003). Crystallization *Physical Chemistry of Foods* (pp. 601-667): CRC Press.

Size: 21.6350 mg

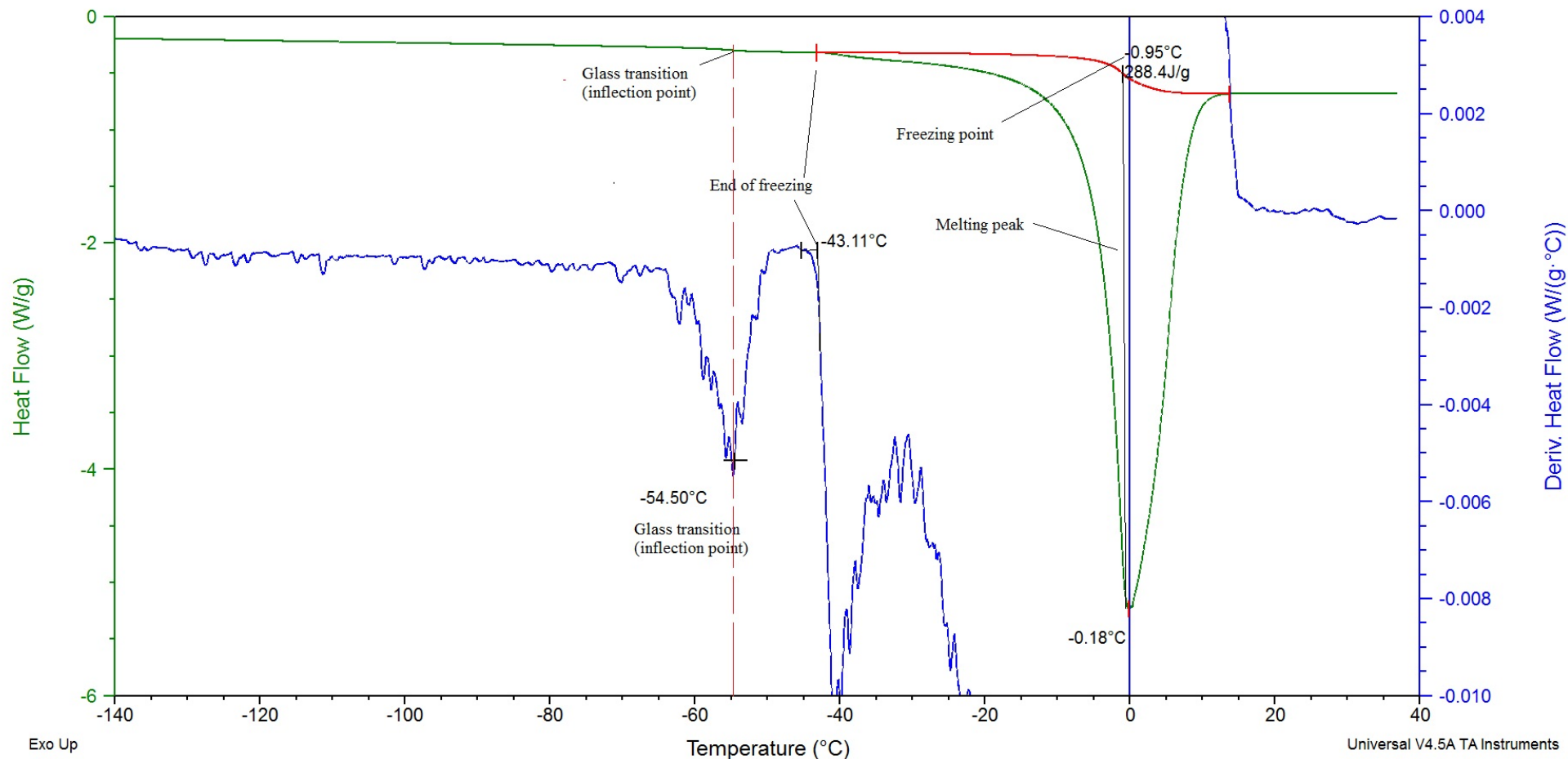
**DSC**



Organic fresh apples, DSC-curve, heat flow curve (green) and derived heat flow curve (blue)

Size: 15.9380 mg

**DSC**

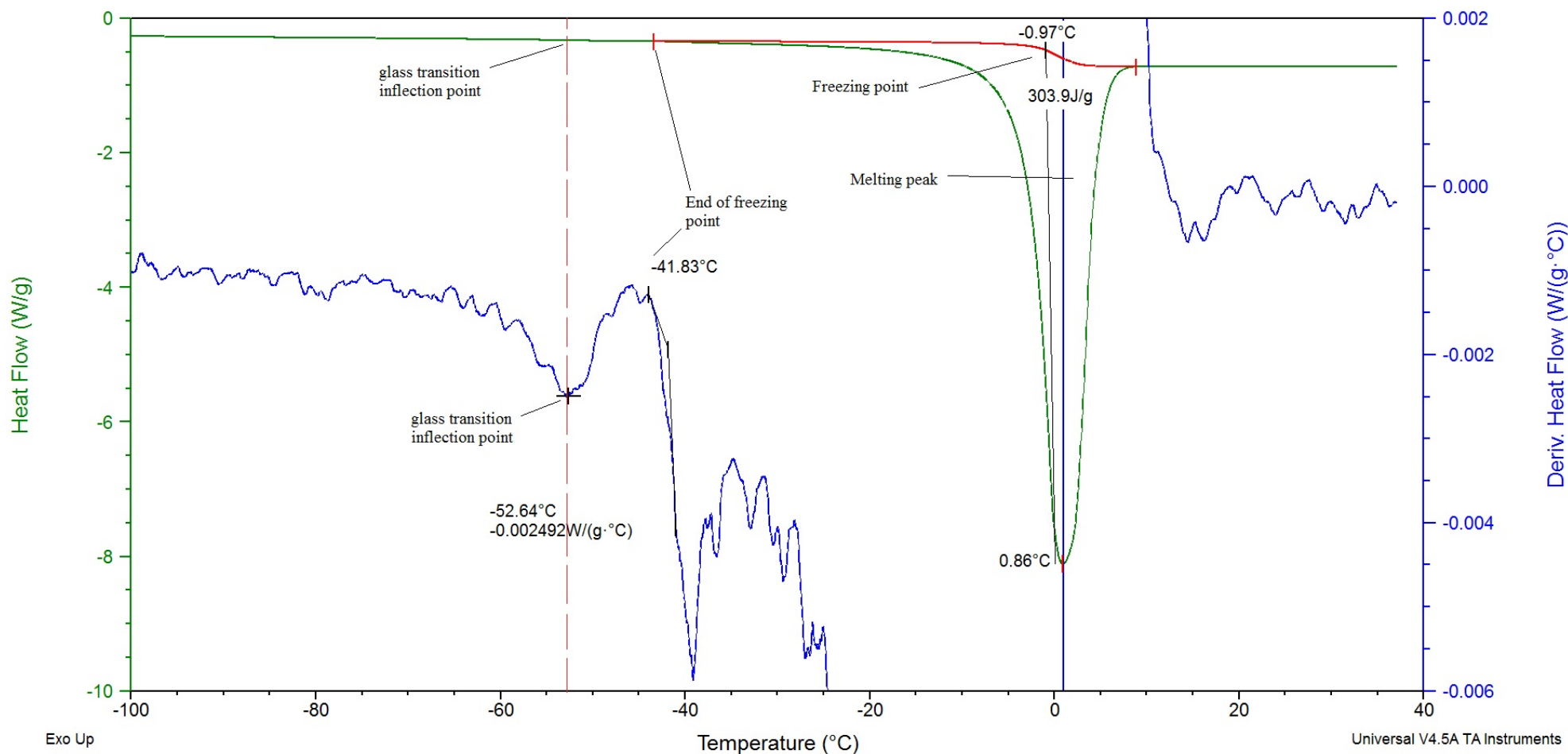


Non-Organic fresh apples, DSC-curve, heat flow curve (green) and derived heat flow curve (blue)



Size: 5.5440 mg

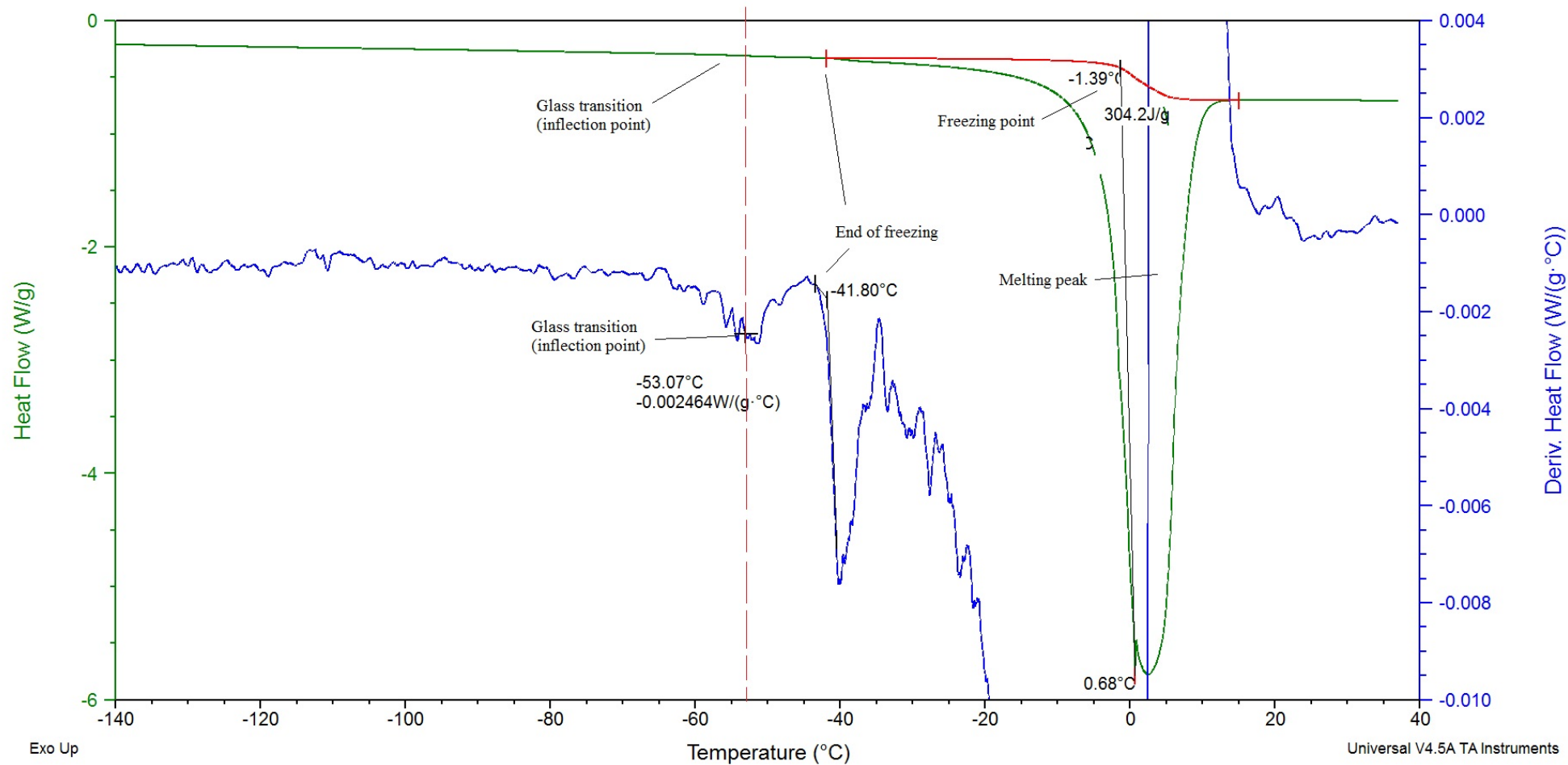
**DSC**



Organic carrots skin, DSC-curve, heat flow curve (green) and derived heat flow curve (blue)

Size: 10.4070 mg

DSC

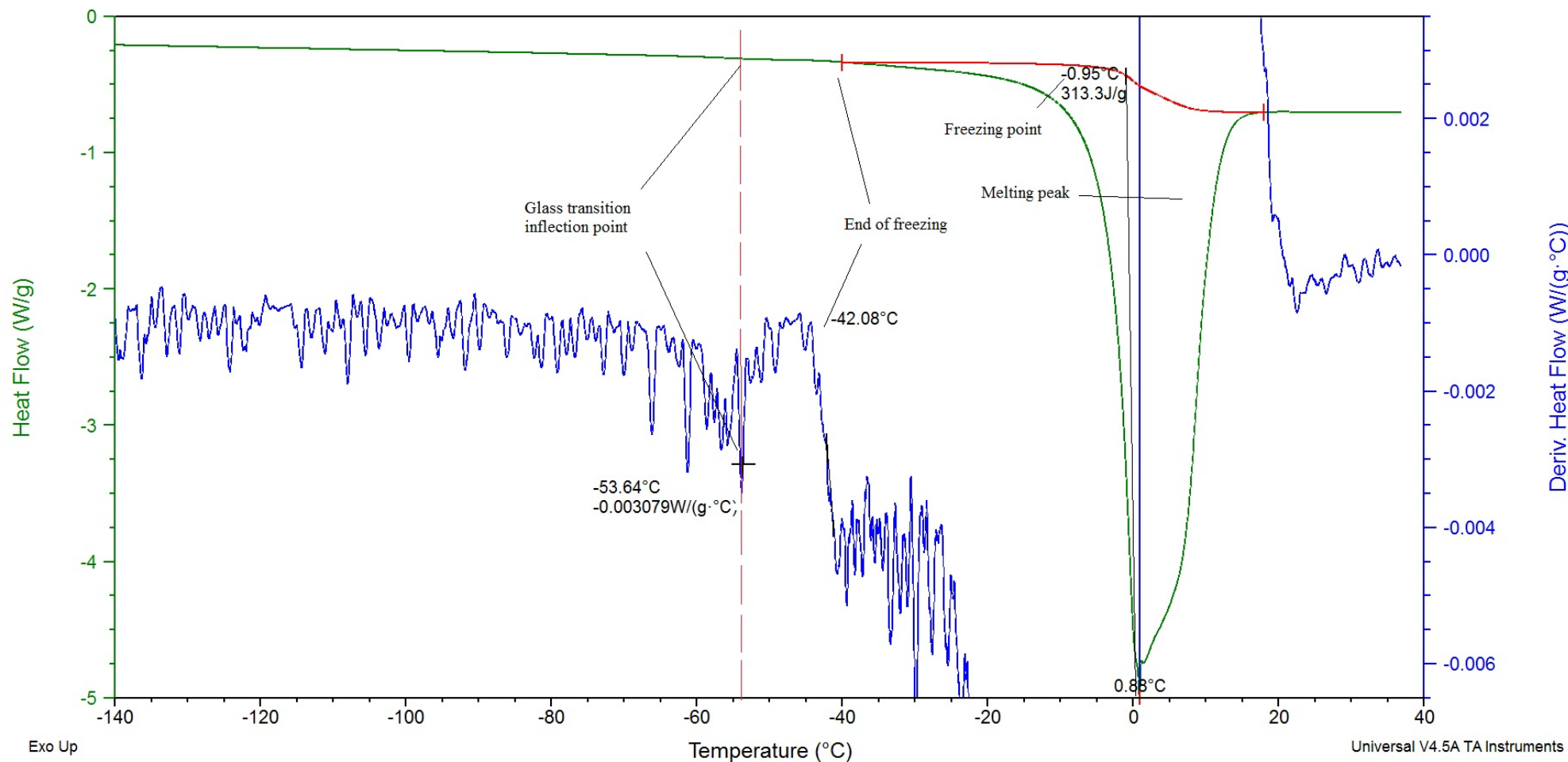


Organic carrots main tissues, DSC-curve, heat flow curve (green) and derived heat flow curve (blue)

Sample: OgrCarrot core  
 Size: 15.3460 mg  
 Method: cp  
 Comment: Orgcarrot\_core

**DSC**

File: C:\...\SusOrganic\OrgCarrot\_core.001  
 Operator: Ignat  
 Run Date: 14-Dec-2015 10:50  
 Instrument: DSC Q2000 V24.11 Build 124

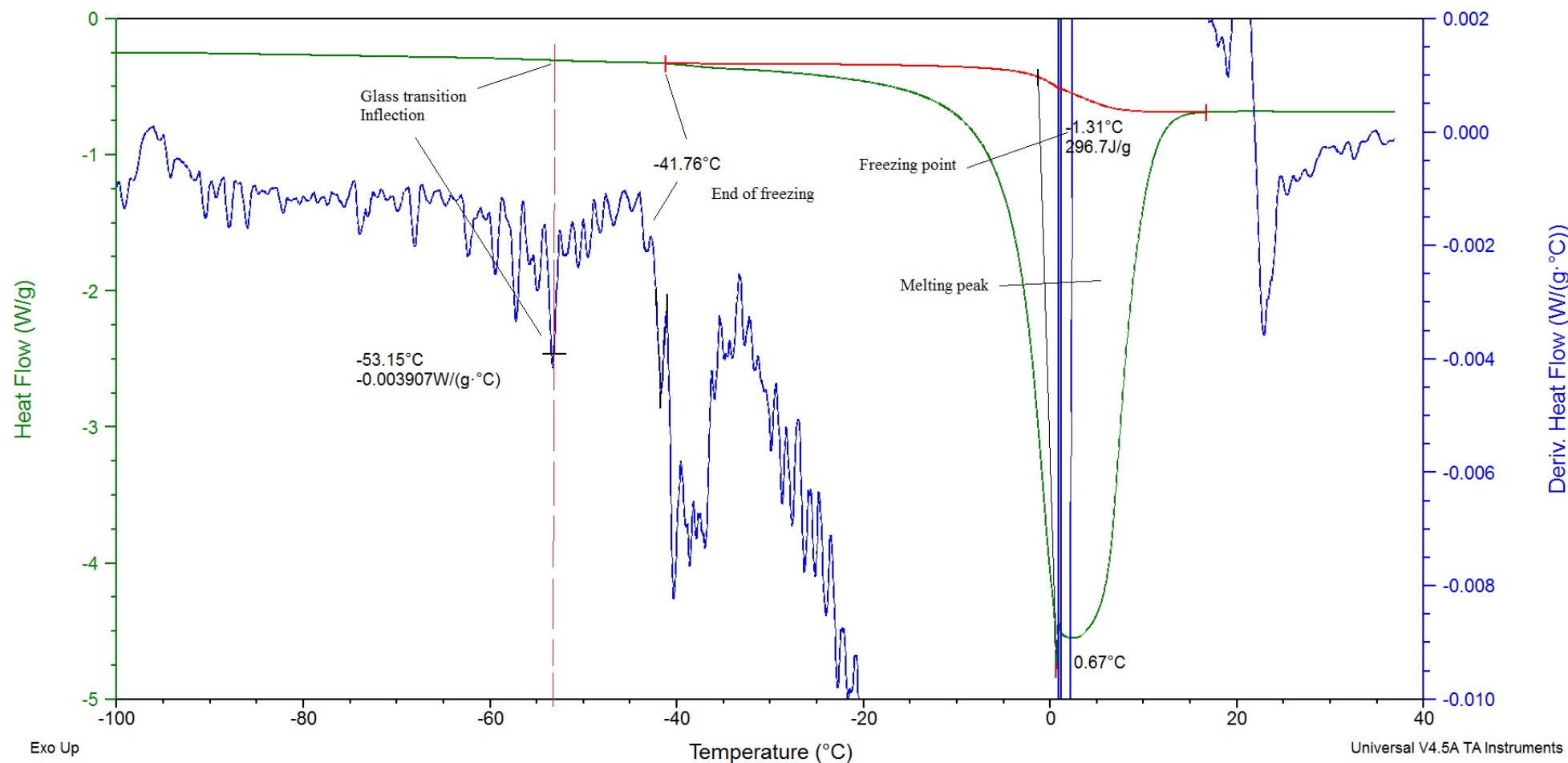


Organic carrots core, DSC-curve, heat flow curve (green) and derived heat flow curve (blue)

Sample: NonOgrCarrot skin  
 Size: 14.8290 mg  
 Method: cp  
 Comment: NonOrgcarrot\_skin

**DSC**

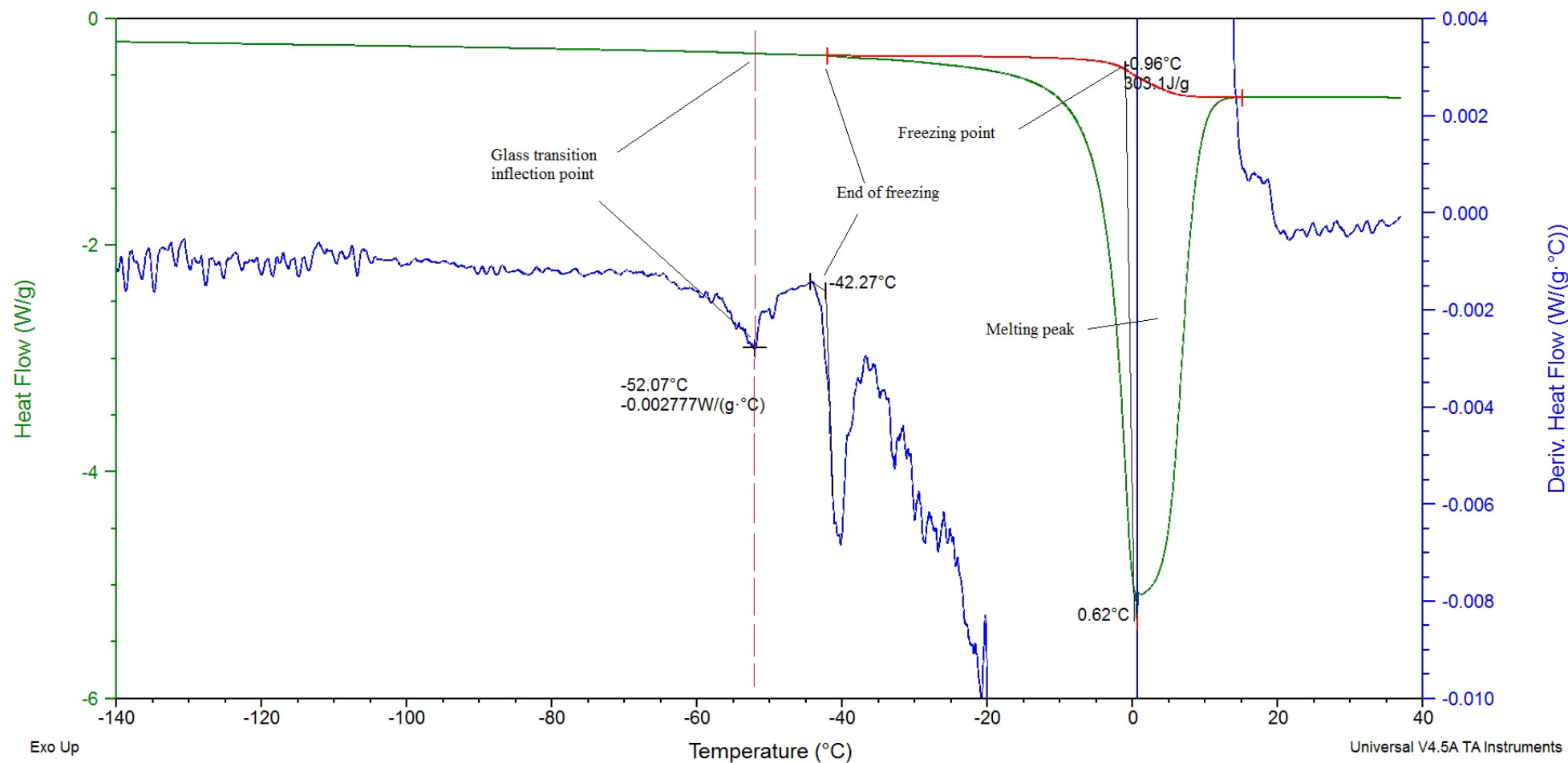
File: C:\...\SusOrganic\NonOrgCarrot\_skin.001  
 Operator: Ignat  
 Run Date: 11-Dec-2015 14:01  
 Instrument: DSC Q2000 V24.11 Build 124



Non-Organic carrots skin, DSC-curve, heat flow curve (green) and derived heat flow curve (blue)

Size: 10.9820 mg

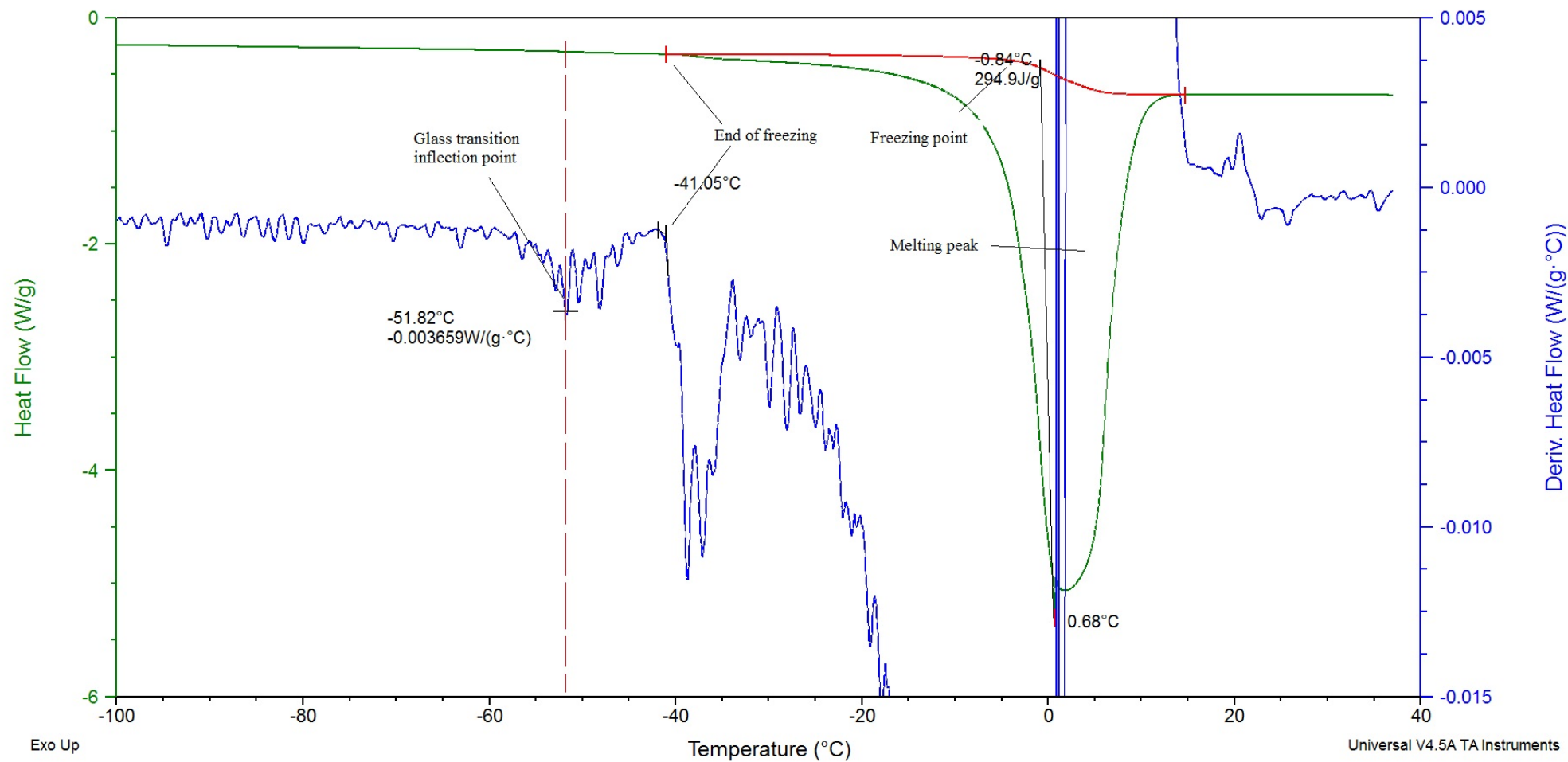
**DSC**



Non-Organic carrots core, DSC-curve, heat flow curve (green) and derived heat flow curve (blue)

Size: 12.5930 mg

**DSC**

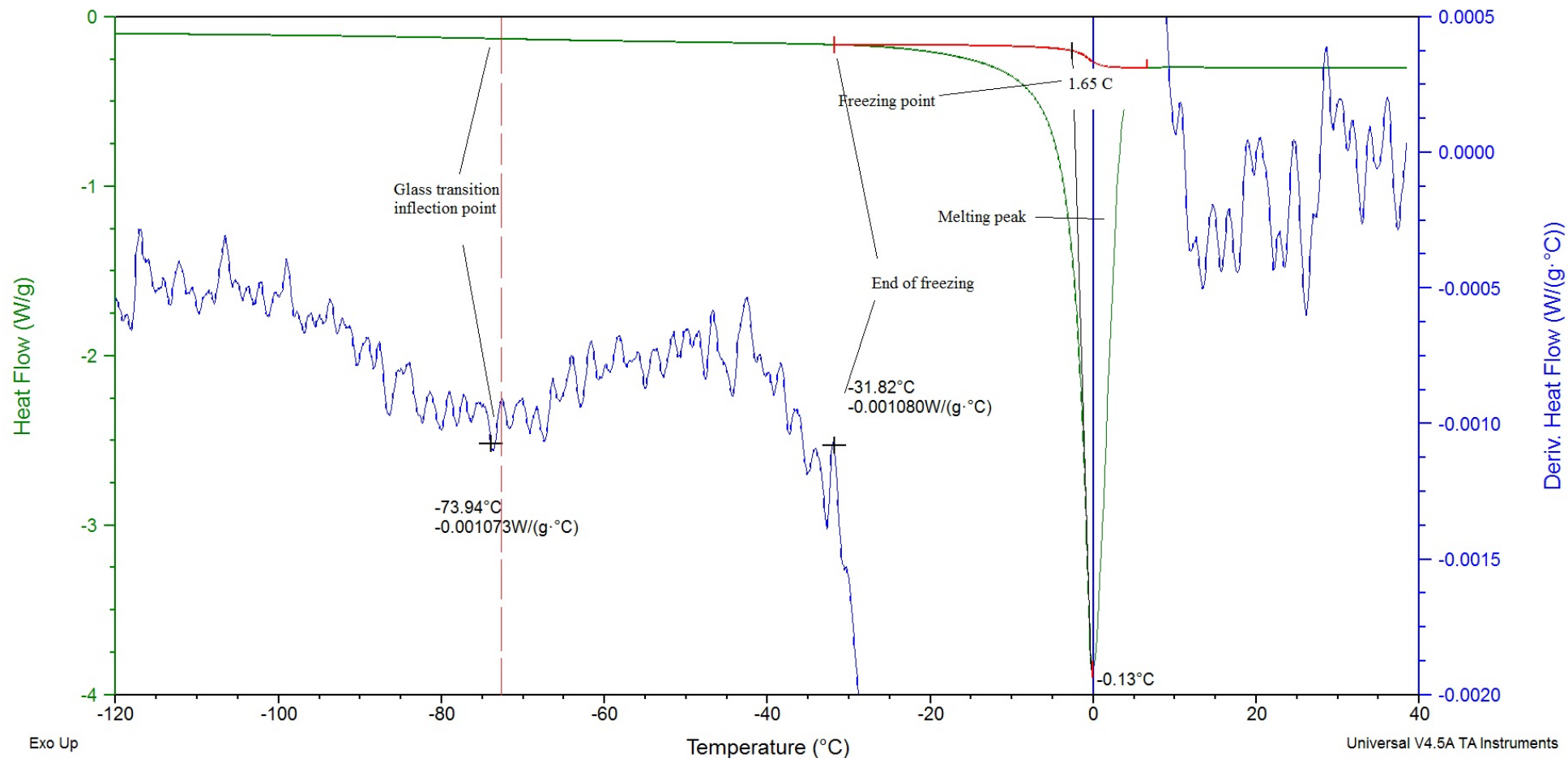


Non-Organic carrots main tissues, DSC-curve, heat flow curve (green) and derived heat flow curve (blue)



Size: 13.1460 mg

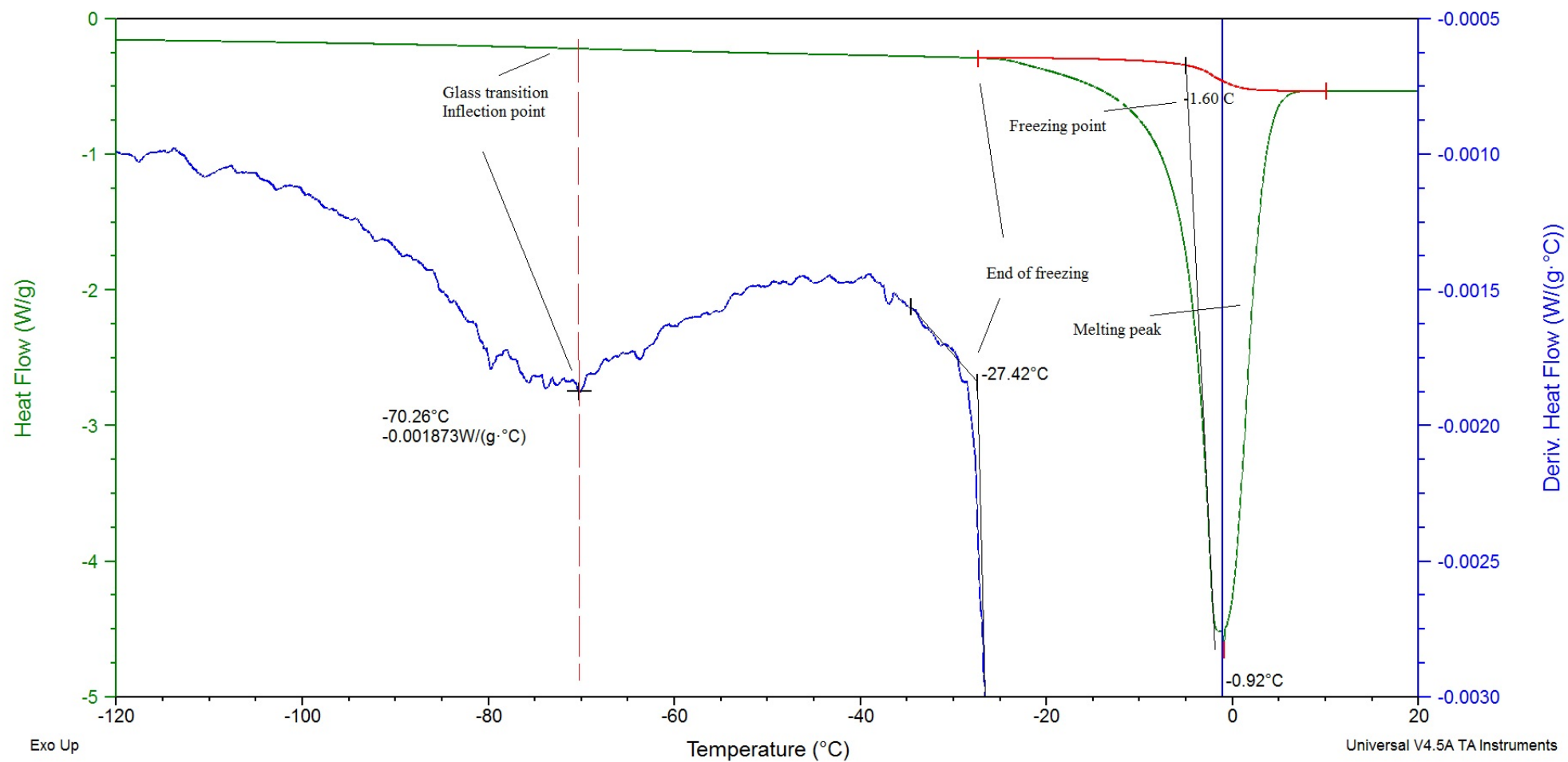
DSC



Organic pork, DSC-curve, heat flow curve (green) and derived heat flow curve (blue)

Size: 10.1080 mg

**DSC**

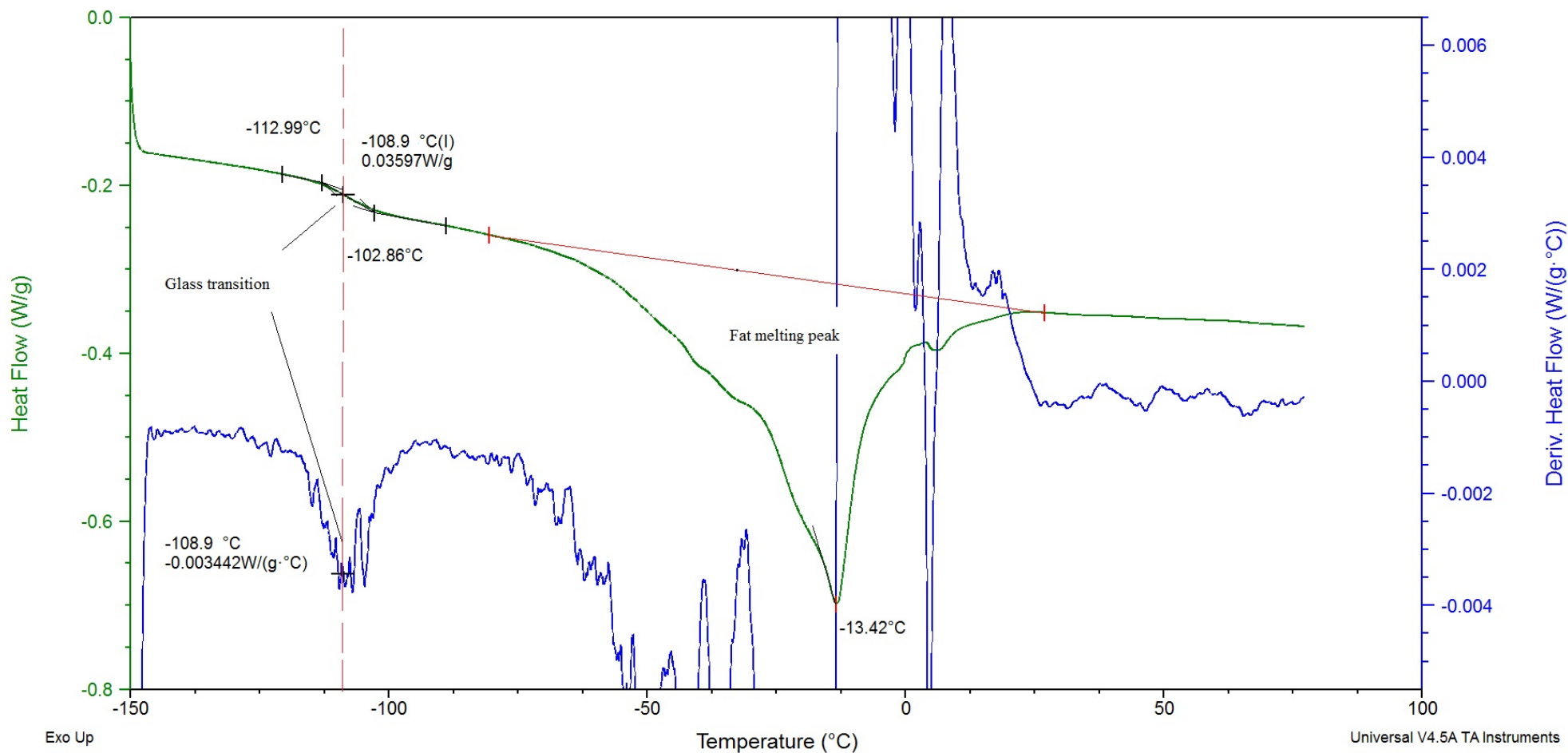


Non-Organic pork, DSC-curve, heat flow curve (green) and derived heat flow curve (blue)

Sample: Org laks  
 Size: 12.0720 mg  
 Method: cp  
 Comment: org laks

**DSC**

File: C:\...\SusOrganic\Organic salmon.001  
 Operator: Ignat  
 Run Date: 26-Nov-2015 14:13  
 Instrument: DSC Q2000 V24.11 Build 124

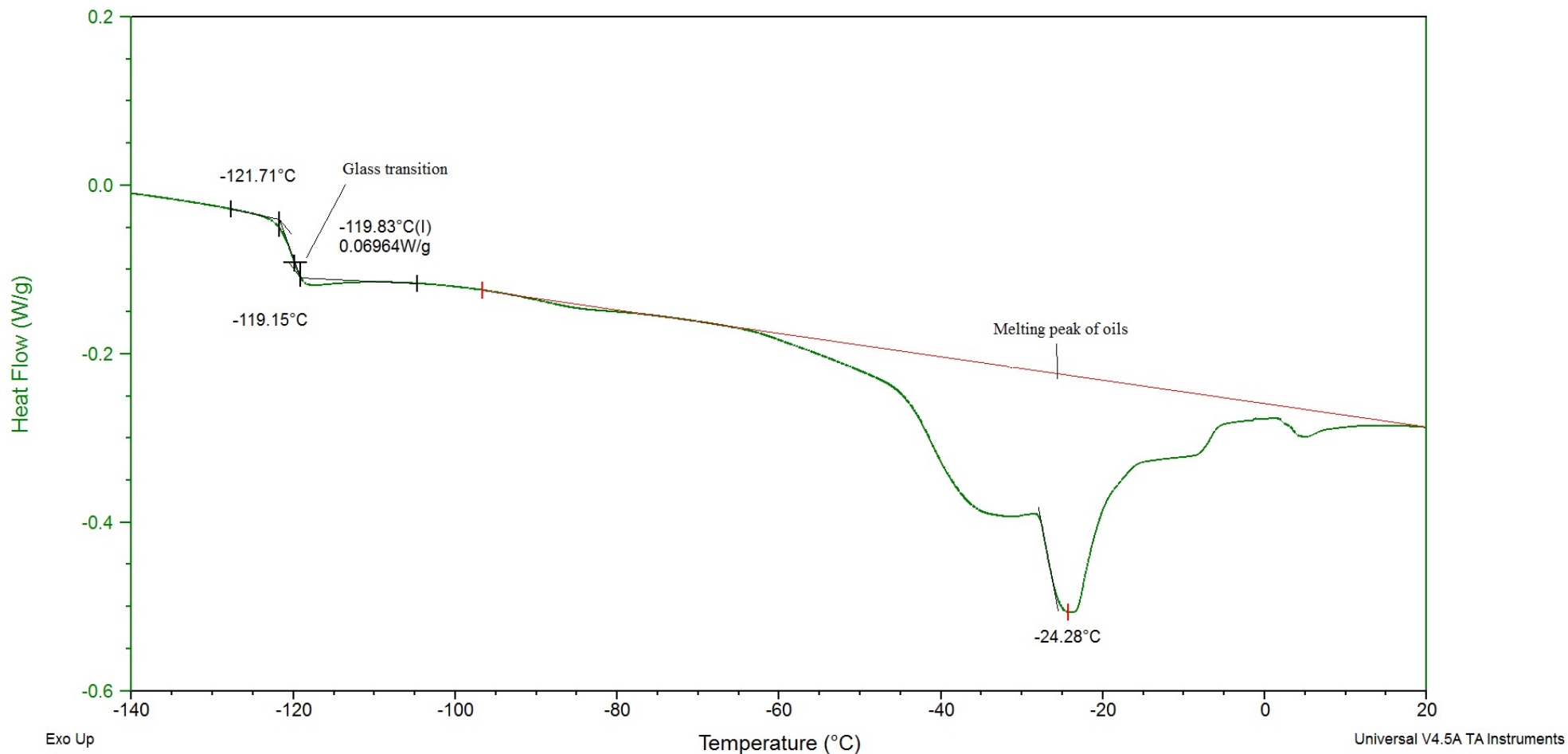


Organic salmon fat melting, DSC-curve, heat flow curve (green) and derived heat flow curve (blue)

Sample: salmon oil\_non\_organic  
 Size: 5.6660 mg

**DSC**

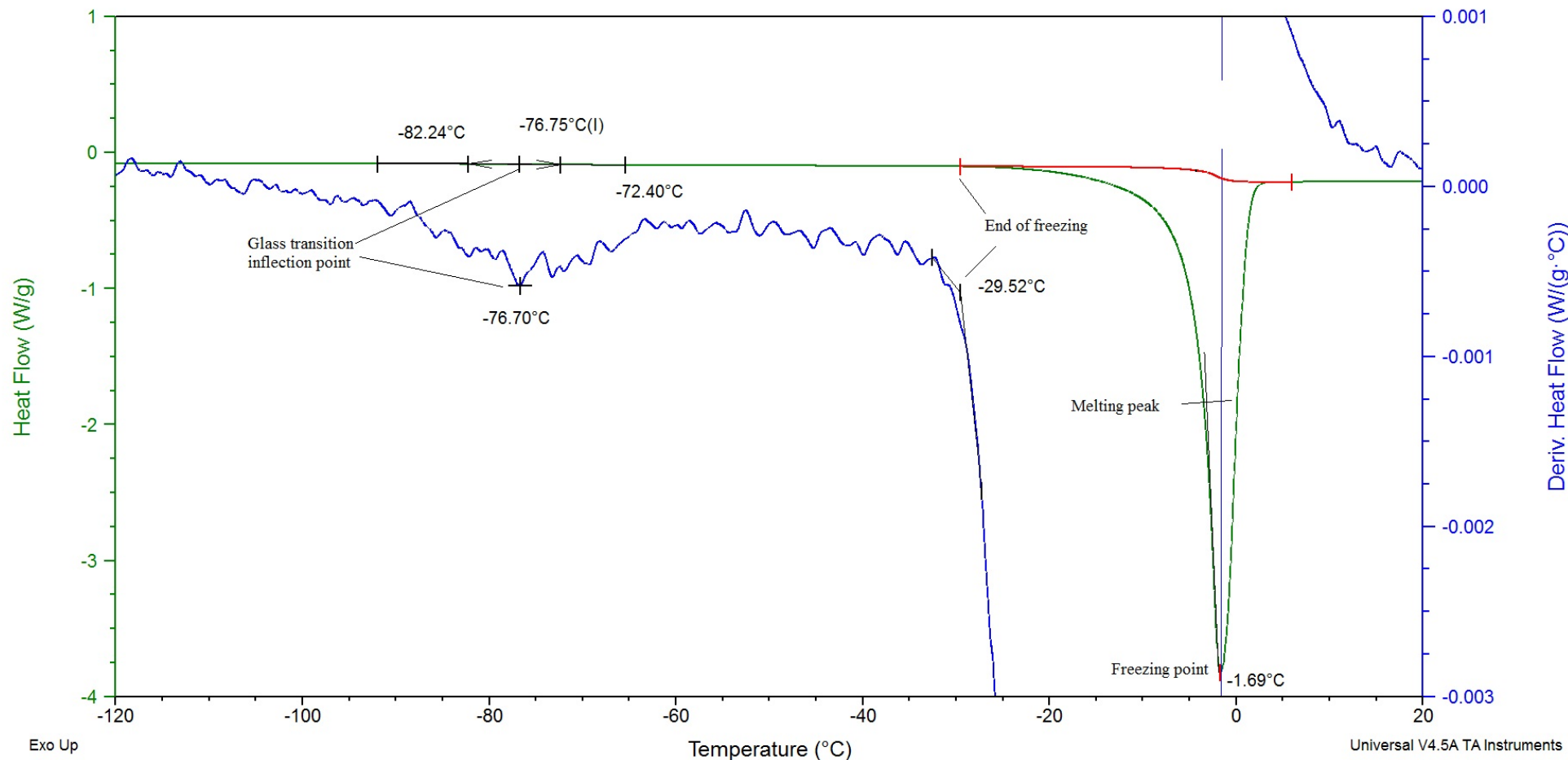
File: C:\...salmon oil\_non\_org.txt  
 Operator: Ignat  
 Run Date: 12-Dec-2015 10:01  
 Instrument: DSC Q2000 V24.10 Build 122



Non-Organic salmon fat melting, DSC-curve, heat flow curve (green)

Size: 8.4910 mg

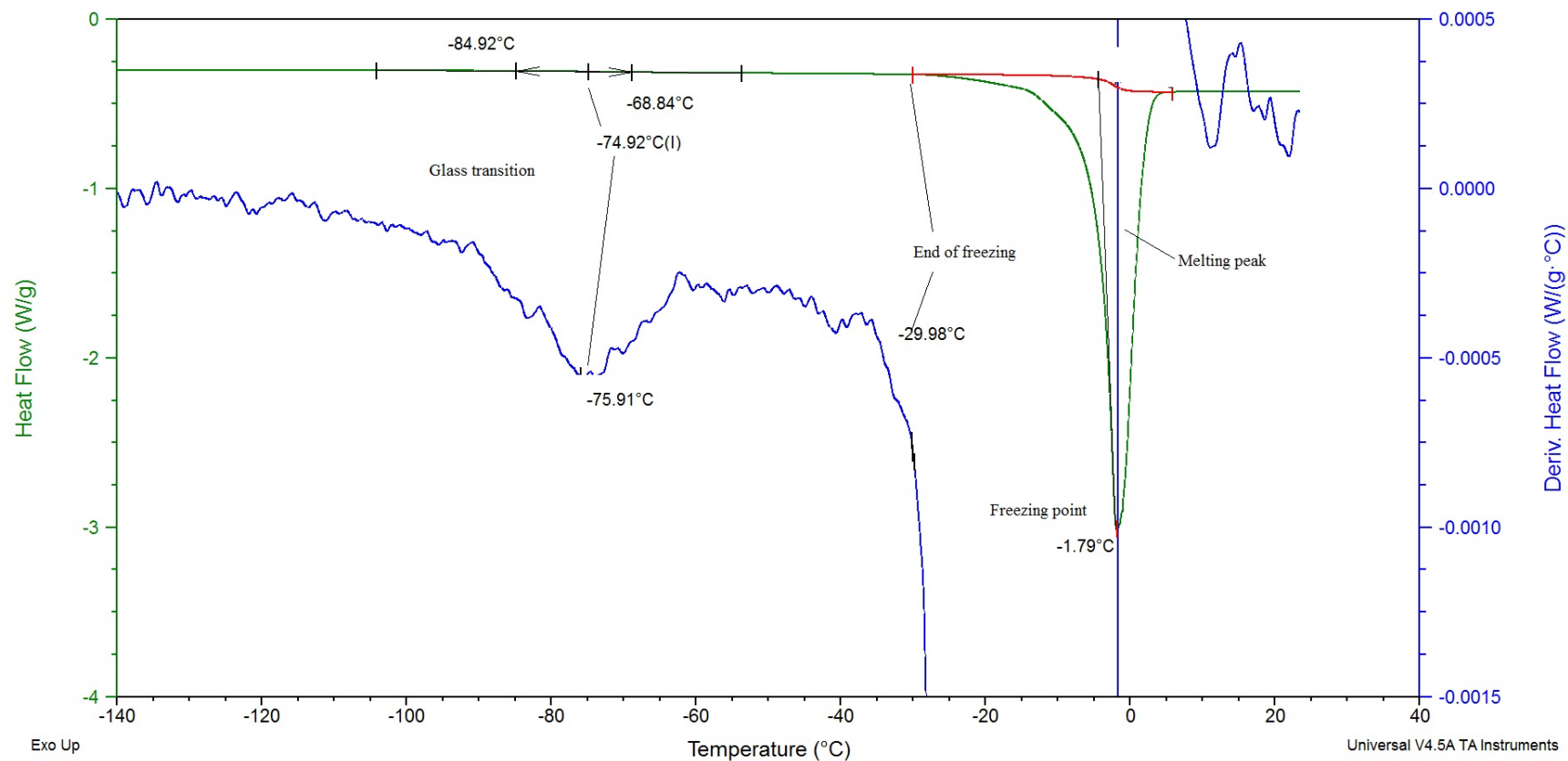
**DSC**



Non-Organic salmon, DSC-curve, heat flow curve (green) and derived heat flow curve (blue)

Size: 17.0210 mg

DSC



Organic salmon, DSC-curve, heat flow curve (green) and derived heat flow curve (blue)



Technology for a better society

[www.sintef.no](http://www.sintef.no)